CHAPTER-II

PREPARATION OF FERRITES

CHAPTER-II
PREPARATION OF FERRITES

SECTION -A

2.1 INTRODUCTION :

Both electrical and magnetic properties of ferrites predominantly depend on density, porosity and microstructure which in turn depend on the method of preparation, purity of starting materials, mixing, sintering temperature and time, partial pressure of oxygen inside the furnace and the rate of cooling. Also, microstructural factors such as grain size, defect concentration, inclusions, pores, grain shape and its orientation, etc, considerably affect the properties of ceramic products. To prepare starting material new methods are developed such as co-precipitation method, freeze drying method and spray roasting method [1].

The ceramic process makes it possible to prepare complex chemical composition, achieve desired microstructure and shape the final product much more economically.

In this chapter a brief review of ceramic process etc. is given. The details of method of preparation of ferrite sample in the laboratory are also given.

2.2 PREPARATION OF FERRITES

In the ceramic process very pure constituents in oxide form are taken in finely divided state. Then, they are thoroughly and uniformally mixed with special technique. This mixture is sintered for prolonged time at specified temperature to

undergo solid state reaction and therefore,the method is usually called as ceramic process. Basically there are four steps in the preparation of ferrite materials .

1) Through mixing of finely divided ingredients taken in stoichiometric proportion

2) Presintering at a temperature slightly less than the solid state reaction temperature.

3) Powdering and pressing to desired shape.

4) Final sintering.

2.3 PREPARATION OF FERRITE COMPOSITION

The general methods for preparation of ferrite compositions are

a) Oxide method

b) Decomposition method

c) Hydroxide method

d) Oxalate method.

2.3(a) OXIDE METHOD :

It requires little chemical knowledge. This is most extensively used in the commercial production of ferrites. High purity oxides of metals in the required proportion for final product are mixed together. They are mixed manually or wet milled with steel balls for few hours. After milling, the mixture is dried, then powdered and passed through the mesh screen. The mixture is calcinated at elevated temperature powdered and dried. It is then pressed it into suitable shape and finally sintered.

2.3(b) DECOMPOSITION METHOD

One may start with salts such as carbonates, nitrates and oxalates instead of using oxides as starting materials. These are mixed in requisite proportion and preheated, usually in air to produce oxides by thermal decomposition. The oxides prepared ' in situ' are known to undergo the solid state reaction more readily [2]. Other details of this method are similar to the oxide method.

2.3(c) HYDROXIDE PRECIPITATION :

Attempts have been made to precipitate simultaneously the required hydroxides from a solution to avoid lengthy milling process involved in dry mixing. The precipitate contains required metal ions in correct proportion and intimately mixed. Knowledge of solubility products of the substance is essential in order to determine the pH value of complete precipitation. Economos [3] established this method for the preparation of ferrites. This method is also applied for the preparation of YIG [4]. Sato [5] and his co-workers [6] prepared ultrafine spinel ferrites by this method.

2.3 (d) OXALATE PRECIPITATION :

Precipitation of metallic oxalates is preferable for some reasons. Precipitation can be carried out by using ammonium oxalate which does not leave any residue after heating. Most metal oxalates have similar crystal structure. Therefore, precipitation tends to produce mixed crystals which contain the metallic cations with correct proportion in which they were present in solution. Thus mixing with correct ratio can be achieved on a molecular scale. If

the precipitation occurs, at widely different rates, mixed crystals do not form uniformly. Careful calcination at temperature of precipitation yields ferrite with particle size less than 1μ m.

2.4 PRESINTERING AND FINAL SINTERING:

The purpose of presintering is to decompose carbonates, oxalates and higher oxides so that there is no evolution of gases during final sintering. It assists homogenization of material and reduces the shrinkage during the final sintering [7]. There is a slow solid state reaction or the reactants are partly activated.

The presintered powder is remilled in an organic medium such as alcohol or acetone and mixed with a binder such as polyvinyl acetate. The dried powder is introduced into a die and subjected to high pressure using a hydraulic press. The compacted material of desired shape is subjected to final sintering at a temperature at which the solid state reaction occurs.

It is found that sintering atmosphere plays an important role in the sintering process. To be sure of exact proportion of metal ions in the final product, careful control of the sintering atmosphere is very important. The partial pressure, of oxygen atmosphere in the furnace must be equal to the equilibrium oxygen pressure, which changes with temperature of the ferrite, in order to maintain the stoichiometry and the desired valance state.

2.5 MECHANISM OF SOLID STATE REACTION :

In order to get a reliable final product it is necessary to take into account the phase equilibrium of the system during final sintering. During the formation of

ferrites the solid state reaction may be regarded as diffusion of divalent metal oxide MO and iron oxide Fe_2O_3. At the beginning, there is only one phase boundary between these two reactants. Once the nucleation of ferrite MFe_2O_4 occurs, there appear two more phase boundaries, viz. (a) between MO and the ferrite MFe_2O_4 and (b) between Fe_2O_3 and MFe_2O_4. At this stage, further progress of the reaction can only take place by transport of reactants through the ferrite phase.

There are three possible mechanisms

(I) Wagner [8] suggested counter diffusion in which the oxygen ions remain essentially stationary and only cations migrate in opposite directions.

(ii) Even anions can migrate, and the diffusion of cations is compensated by an associated flux of anions O^{2-} instead of counter-current of another cation.

iii) Iron in reduced state, Fe^{2+}, may diffuse through the ferrite layer. During such a process oxygen in gaseous phase is transported; it is given off at MFe_2O_4/Fe_2O_3 interface and it is taken up again at MO/MFe_2O_4 boundary.

All mechanism are possible and perhaps one may predominate but no conclusive remark can be made. Recently, the reaction mechanism in Ni-Zn ferrites was investigated by Parikor et al [9] with the starting ingradients NiO, ZnO and Fe_2O_3 using electron probe X-ray analysis. They found that the ferrite crystallises only on iron oxide. According to these authors, the interaction of NiO and ZnO with Fe_2O_3 takes place by interdiffusion of Fe^{3+}, Fe^{2+} and Ni^{2+}, Zn^{2+}

along with a current of electrons and oxygen ions directed to the ferrite/Fe_2O_3 interface.

2.6 PREPARATION OF FERRITE SAMPLES :

2:6(a) GENERAL FORMULA

The ferrite samples were prepared by the usual ceramic method starting with oxides and carbonates. The general formula of ferrite samples is,

$$Cu_{0.5}Co_{0.5}Cr_xFe_{2-x}O_4$$

where x = 0.0, 0.2,0.4,0.6,0.8 and 1.0

2.6(b) METHOD OF PREPARATION :

A.R. grade oxides : CuO, Fe_2O_3,Cr_2O_3 and cobalt carbonate $CoCO_3$ were used. These oxides and carbonate were weighed in required mole proportions on single pan semimicrobalance having least count of 0.001 gm and were mixed thoroughly in an agate-mortar with acetone. This mixture was dried in an oven at 100°C The dry mixtures were then transferred into alumina crucibles and were presintered at 450°C for 10 hours in a globar furnace. Then the furnace was cooled slowly. The temperature of the furnace was measured with the help of pre-calibrated chromel-alumel thermocouple. The pre-sintered powder was then grounded in agate morter in acetone medium for four hours dried and the fine powder collected in a clean glass tube.

About two grams of this dry powder was then transferred into a die having 1.5 cm diameter and pressed using a hydraulic press to a pressure of the order of 8 tonnes per square inch for about 5 minutes. After removing the load, pellet was taken out from the die.

The pellets thus formed were placed on a platinum foil and kept in a globar furnace and sintered at 950°C for about 24 hours in air for to allow the completion of solid state reaction. Then the furnace was cooled at a rate of 75°C per hour.

For X-ray diffraction studies, the pellets were again ground in a ball mill. Some pellets were reserved for resistivity and magnetisation measurements.

2.7 DENSITY MEASUREMENT :

The densities of the samples were determined by liquid immersion method [10]. For this measurement tolune was used. The measured densities for the system are listed in Table (2.1). The porosity of the samples was calculated by using formula,

$$P = \frac{dx-ds}{dx} \times 100$$

where

$$dx = \frac{8M}{Na^3}$$

where ds - is the actual density calculated by liquid immersion method,

M - is the molecular weight,

a - is the lattice constant, and

N - is the Avogadro's number.

The values of porosity and X-ray densities are also listed in the Table(2.1).

PART-B

X-RAY DIFFRACTION STUDY

2.8 INTRODUCTION :

The study of crystal structure by X-ray diffraction was first made in the year 1912 by Bragg [11]. This technique plays an important role in ferrite research to confirm the structure and the completion of solid state reaction.

2.9 DIFFRACTION METHOD :

The experimental diffraction methods are

1) Laue method
2) Rotating crystal method
3) Powder method

Following is a brief description of the X-ray diffractometer and its principle.

The principle of this method and main features are shown in Fig.2.1. In this method, a beam of X-rays is allowed to pass through the slit A of the collimeter. As crystals are randomly oriented, a reflection at particular angle θ is due to a set of atomic planes which satisfy Bragg's condition. With the help of special slit 'B' the diffracted beam is collimated. It is then converged and focused at a slit F and allowed to enter the coutner G. The counter G is connected to a count rate meter whose output is fed to a fast automatic recorder which registers counts per second versus 2θ. The location of the centroid of the recorded peak gives the corresponding Bragg's angle, $2\theta_{hkl}$. The reciprocal lattice lies on the surface cf radicles (hkl) and is oriented for

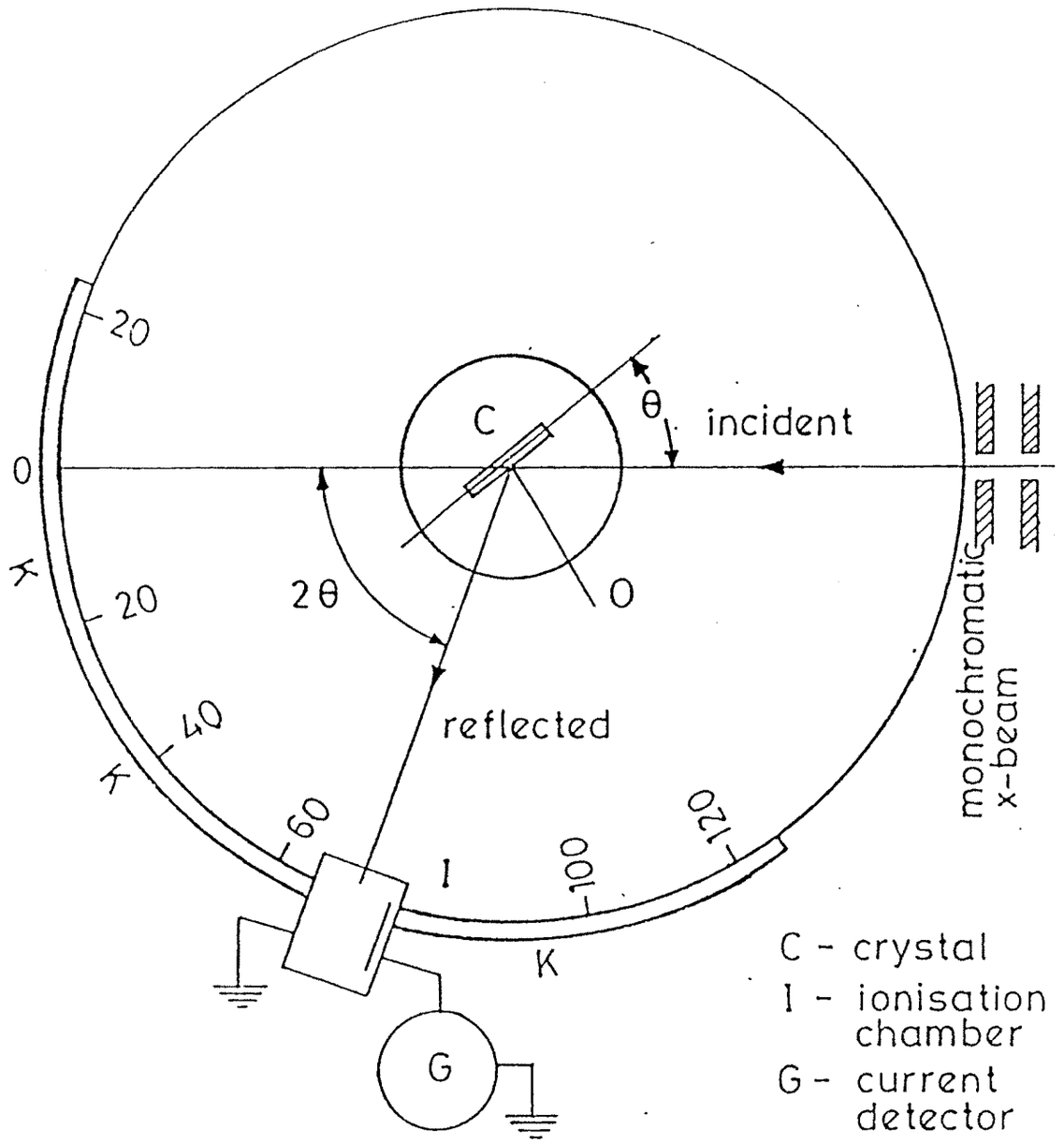
20
0
K
20
40
K
60
2θ
C
θ
incident
O
reflected
monochromatic
x-beam
I
100
120
K
C - crystal
I - ionisation chamber
G - current detector
G

Fig. 2.1

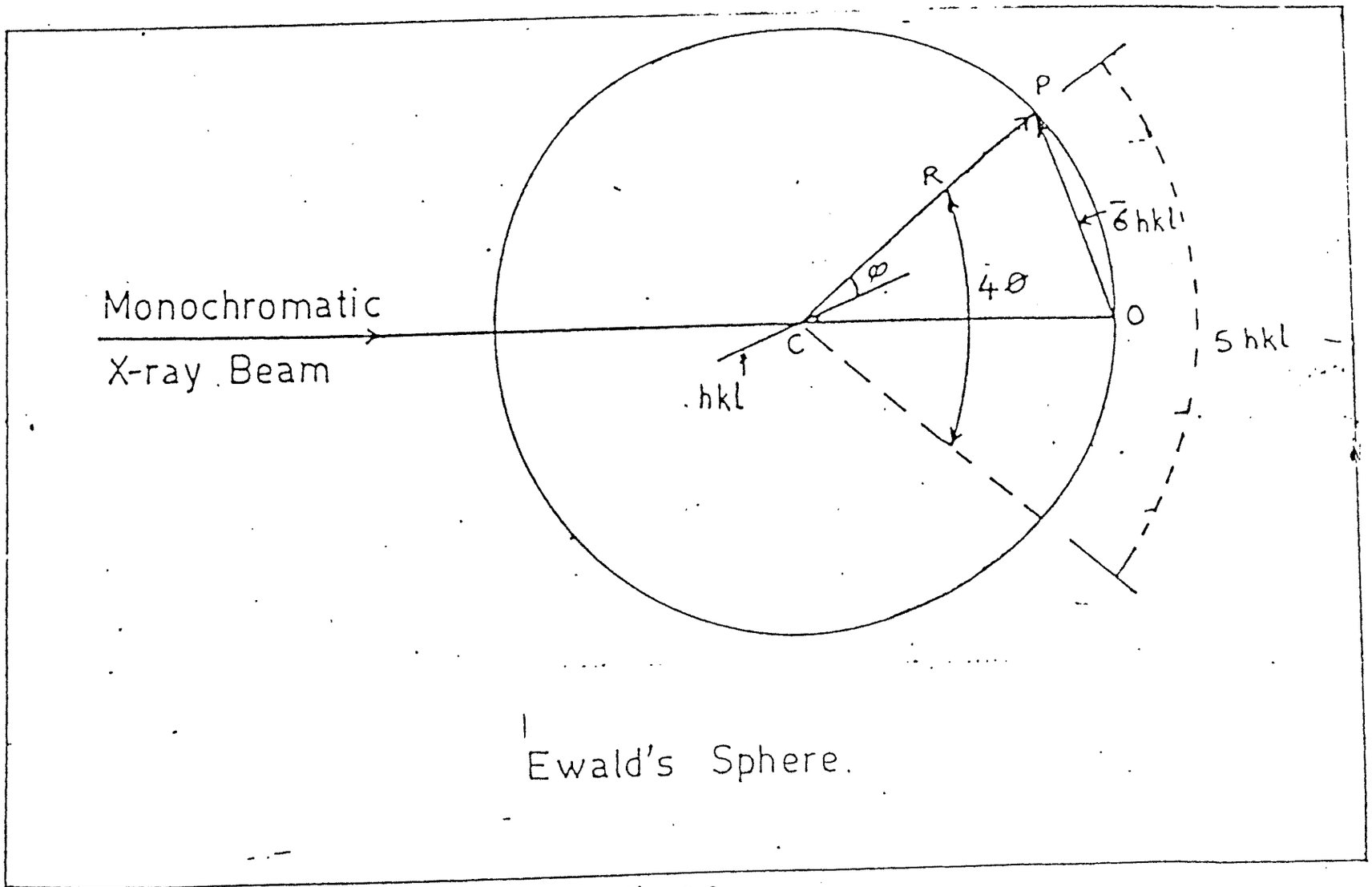

Fig. 3.2

every possible value of hkl cutting the Ewald's sphere as shown in Fig.2.2. By geometry of Ewald's sphere.

$$\Delta\theta_{hkl} = \frac{S_{hkl}}{R} \qquad \ldots\ldots(2.1)$$

$$\therefore \quad \theta_{hkl} = \frac{S_{hkl}}{4R} \qquad \ldots\ldots(2.2)$$

Using Bragg's law, we have,

$$2\, d_{hkl}\, \mathrm{Sin}\theta_{hkl} = n\lambda \qquad \ldots\ldots(2.3)$$

where n the order of reflection

The interplaner spacing d_{hkl} can be calculated.

The receiving slit and counter are supported on the carriage E which can be rotated about the vertical axis through C whose angular position 2θ can be read on circular scale K as counter moves through 2θ degrees between E and H. However, modern X-ray diffractometer employs scintillation counter and automatic recording of a graph of intensity of X-rays with respect to Bragg angle.

2.10 EXPERIMENTAL X-RAY TECHNIQUE

The X-ray diffraction patterns of the samples were taken by using CuK_α radiation of wavelength 1.5418 A° on Philips X-ray diffractometer (Model-MM 9920). The powder was spread uniformally on a mounted screen of sample holder so as to form a plane surface of the specimen. The speed of chart was 1° per min. and recording was made from 20° to 80° of 2θ . The lattice parameter for each cubic spinel ferrite sample was determined using the following procedure.

From the chart the peak values are recorded and their corresponding d values are calculated from Bragg's law

$$2d \sin\theta = n\lambda \qquad \text{.....(2.4)}$$

and also by using the relation [12]

$$d\,cal = \frac{a}{\sqrt{h^2 + k^2 + l^2}} \qquad \text{.....(2.5)}$$

where 'a' is lattice constant

The following equations are used to calculate the bond length of tetrahedral (R_A) and octahedral (R_B) sites.

$$R_A = (u - 1/4)\, a.\sqrt{3} \qquad \text{.....(2.6)}$$

$$R_B = (5/8 - u)\, a \qquad \text{.....(2.7)}$$

where u is oxygen parameter

As peak is observed in diffraction pattern the Bragg's law must be obeyed.

$$2d \sin\theta = \lambda \qquad \text{.....(2.8)}$$

$$2\left(\frac{a}{\sqrt{(h^2 + k^2 + l^2)}}\right) \sin\theta = \lambda \qquad \text{.....(2.9)}$$

squaring and rearranging we get

$$\frac{\sin^2\theta}{h^2 + k^2 + l^2} = \frac{\sin^2\theta}{S} = \frac{\lambda^2}{4a^2} \qquad \text{.....(2.10)}$$

where

$$S = h^2 + k^2 + l^2$$

The sum 'S' is always an integer and the term $\lambda^2/4a^2$ must be constant for given pattern, the equation (2.10) helps in indexing the pattern. For this we consider a prominent (311) line of the diffraction pattern as it is easily identified in XRD pattern of a cubic spinel. From its corresponding value of 2θ , $\sin^2\theta$ is determined. Hence lattice parameter 'a' can be determined using the equation (2.10) for (311) plane.

This lattice parameter 'a' is then used for indexing the other planes using and sin fopr that plane. In this type of indexing , $h^2 + k^2 + l^2$ is determined from the equation (2.10) for different values of for which maxima have appeared. The integral sum $h^2 + k^2 + l^2$ is used to find (h,k,l).

2.11 RESULTS AND DISCUSSION

X-ray diffractograms records of slow cooled $Cu_{0.5}Co_{0.5}Cr_xFe_{2-x}O_4$ are shown in Fig.2.3a,b,c,d,e,f. The diffraction maxima were indexed by G.C.F. method as explained else where and were checked and tallied with standard ones for spinel structure [12,13].

The reflections for cubic structure are observed for the planes (220), (311), (400), (422), (511) and (440). These planes are allowed ones for spinel structure. The d values of the samples ($Cu_{0.5}Co_{0.5}Cr_xFe_{2-x}O_4$) for (x=0.0,0.2,0.4,0.6,0.8 and 1.0) are represented in the inset table in respective diffraction patterns. The calculated d values of the samples are in close agreement with the observed ones indicating clearly that the ferrites prepared are fully formed with cubic spinel structure.

Sample $Cu_{0.5}Co_{0.5}Fe_2O_4$

Plane hkl	220	311	400	422	511	440
d_{obs} (Å)	2.9656	2.5295	2.0957	1.7107	1.6137	1.4824
$d_{cal.}$ (Å)	2.9661	2.5295	2.0974	1.7125	1.6145	1.4830

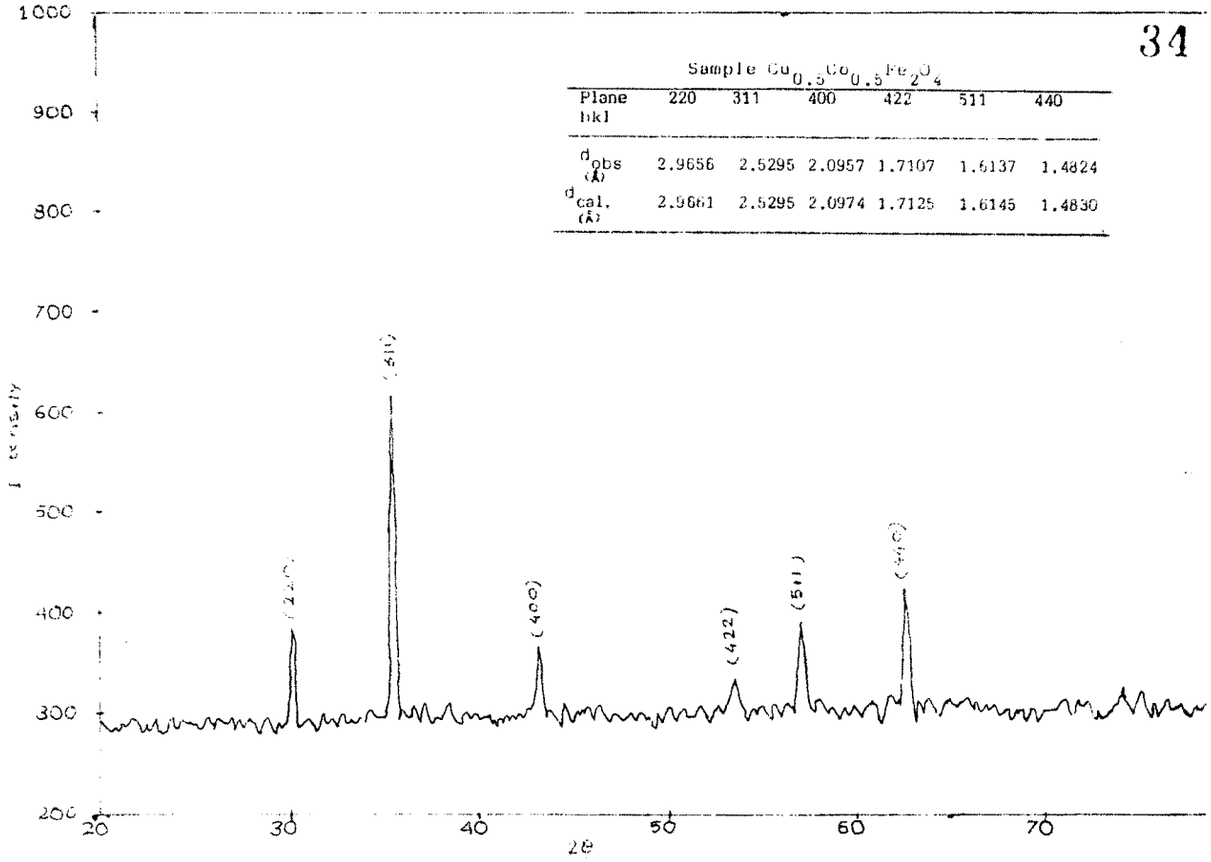

2.3(a) X-ray Diffraction Pattern for the Sample $Cu_{0.5}Co_{0.5}Fe_2O_4$

sample $Cu_{0.5}Co_{0.5}Cr_{0.2}Fe_{1.8}O_4$

Plane hkl	220	311	400	422	511	440
$d_{obs.}$ (Å)	2.9584	2.5226	2.093	1.7089	1.6102	1.4793
$d_{cal.}$ (Å)	2.9580	2.5226	2.0916	1.7078	1.6101	1.4790

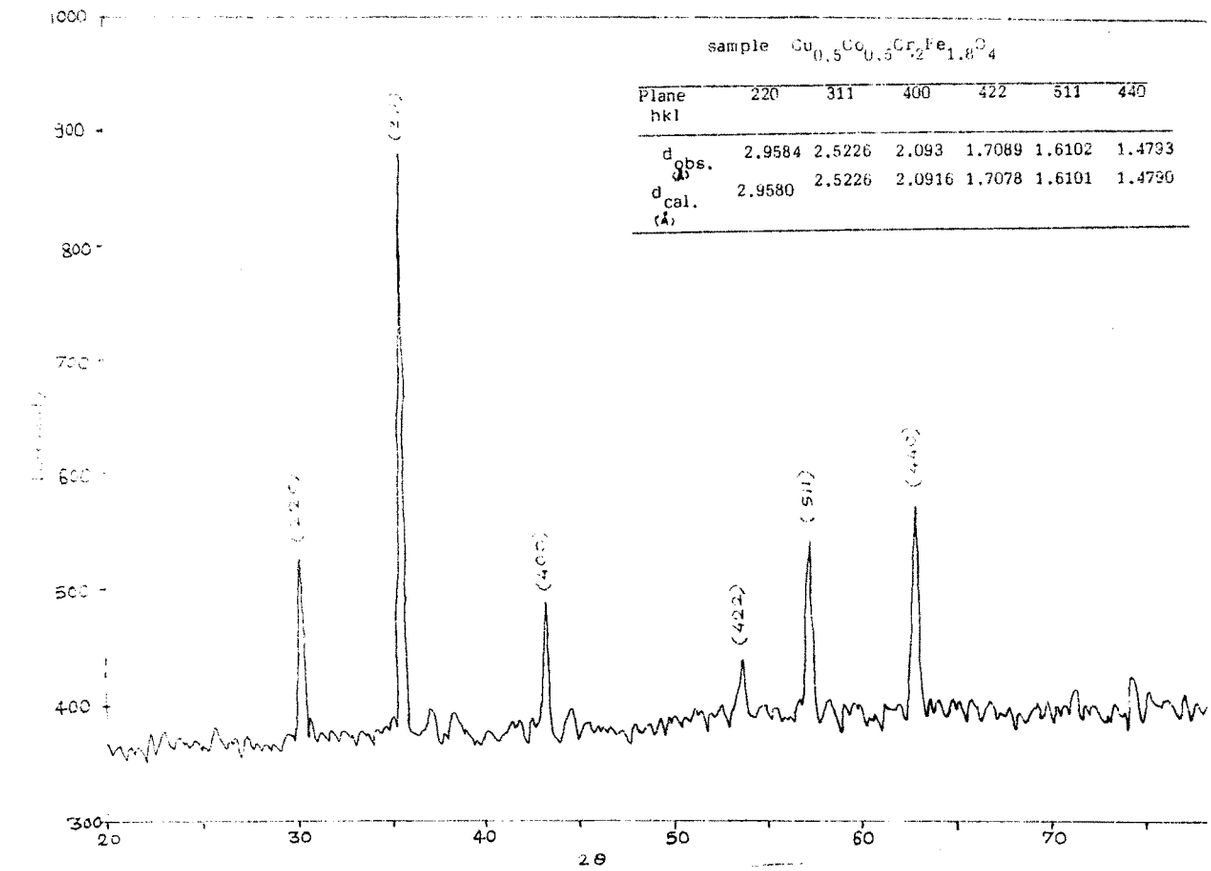

2.3(b) X-ray Diffraction Pattern for the Sample $Cu_{0.5}Co_{0.5}Cr_{0.2}Fe_{1.8}O_4$

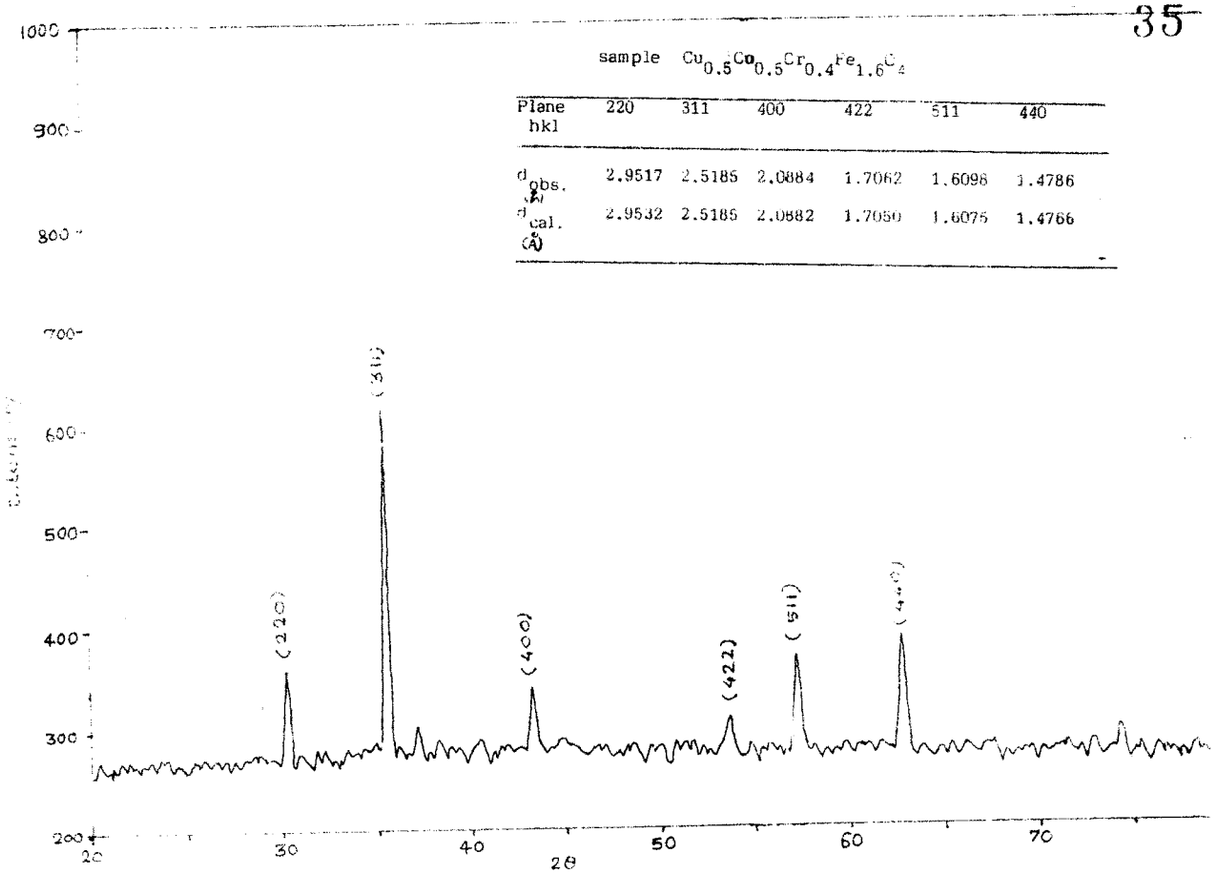

sample $Cu_{0.5}Co_{0.5}Cr_{0.4}Fe_{1.6}O_4$

Plane hkl	220	311	400	422	511	440
$d_{obs.}$ (Å)	2.9517	2.5185	2.0884	1.7062	1.6098	1.4786
$d_{cal.}$ (Å)	2.9532	2.5185	2.0882	1.7050	1.6075	1.4766

2.3(c) X-ray Diffraction Pattern for the Sample $Cu_{0.5}Co_{0.5}Cr_{0.4}Fe_{1.6}O_4$

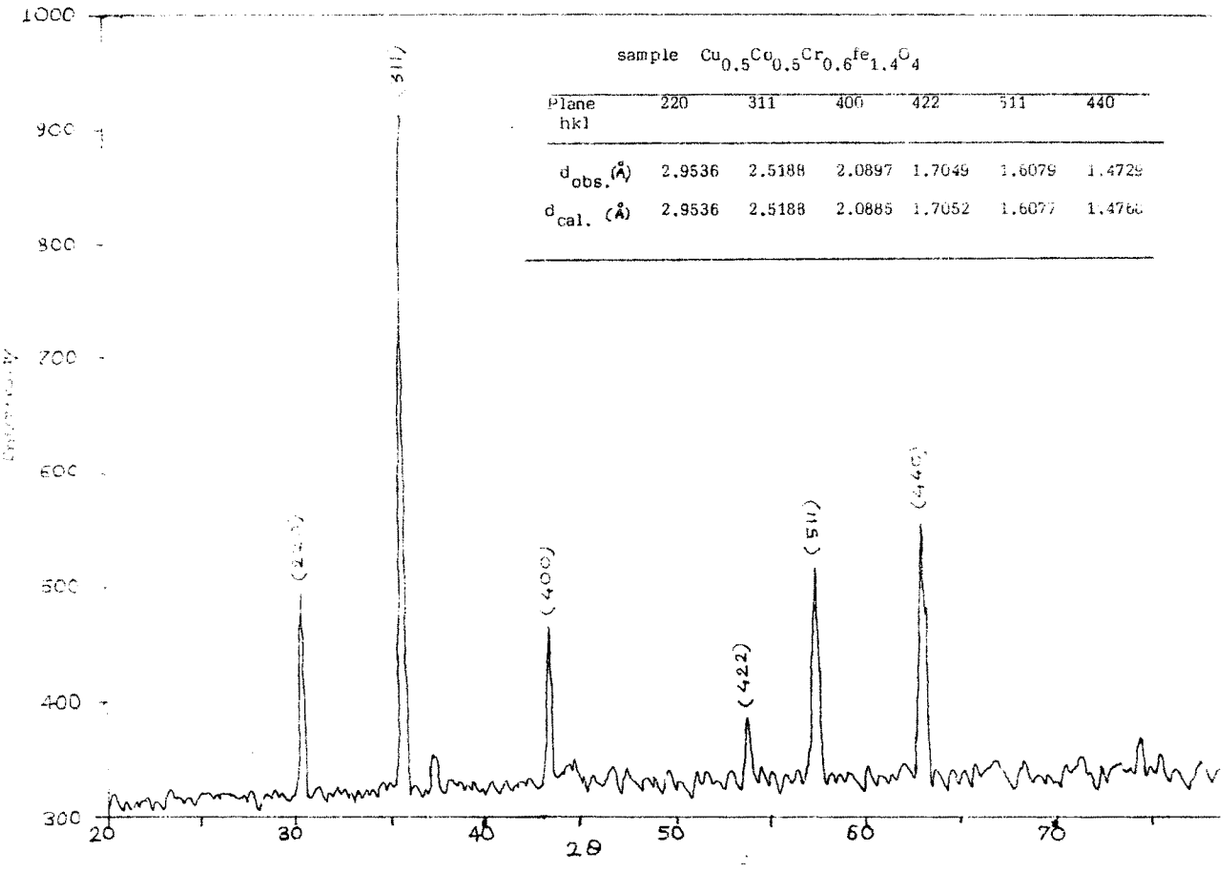

sample $Cu_{0.5}Co_{0.5}Cr_{0.6}Fe_{1.4}O_4$

Plane hkl	220	311	400	422	511	440
$d_{obs.}$ (Å)	2.9536	2.5188	2.0897	1.7049	1.6079	1.4729
$d_{cal.}$ (Å)	2.9536	2.5188	2.0885	1.7052	1.6077	1.4766

2.3(d) X-ray Diffraction Pattern for the Sample $Cu_{0.5}Co_{0.5}Cr_{0.6}Fe_{1.4}O_4$

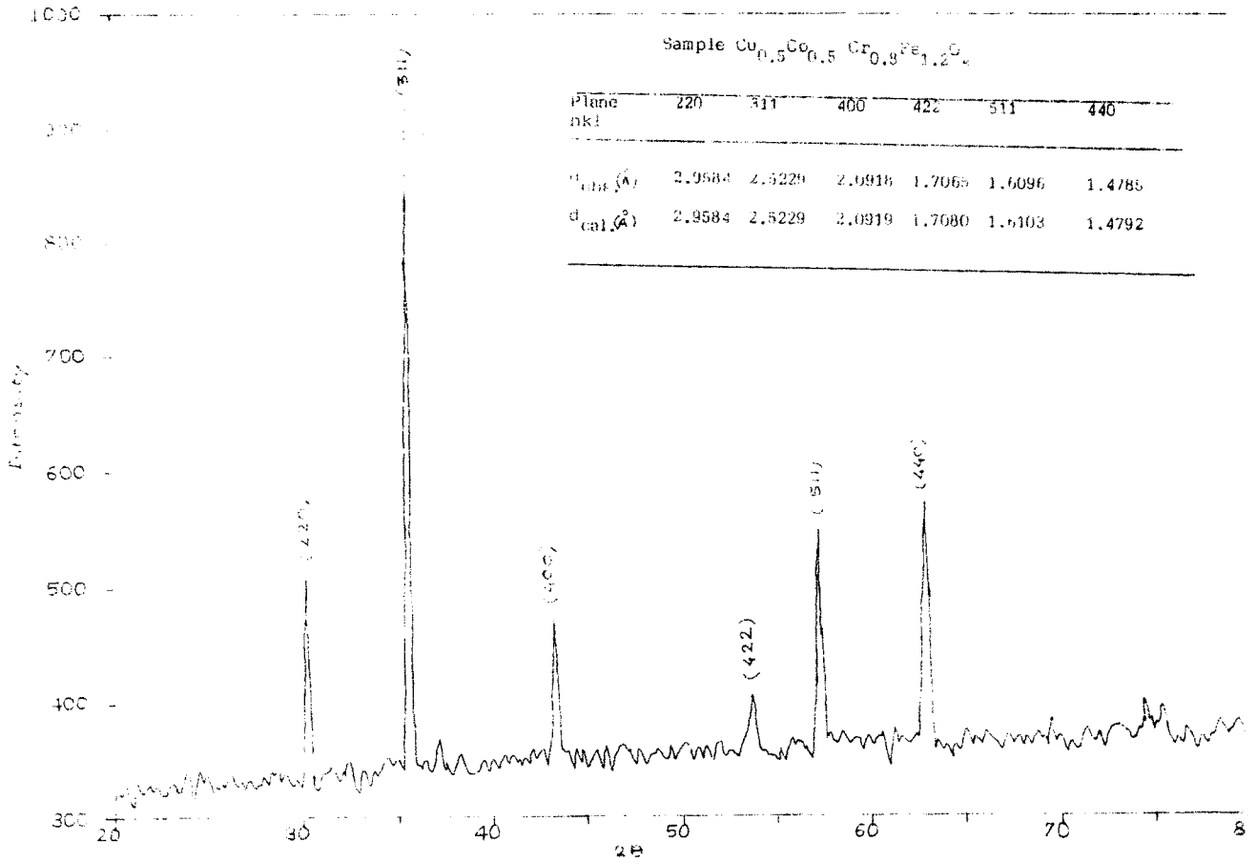

2.3(e) X-ray Diffraction Pattern for the Sample $Cu_{0.5}Co_{0.5}Cr_{0.8}Fe_{1.2}O_4$

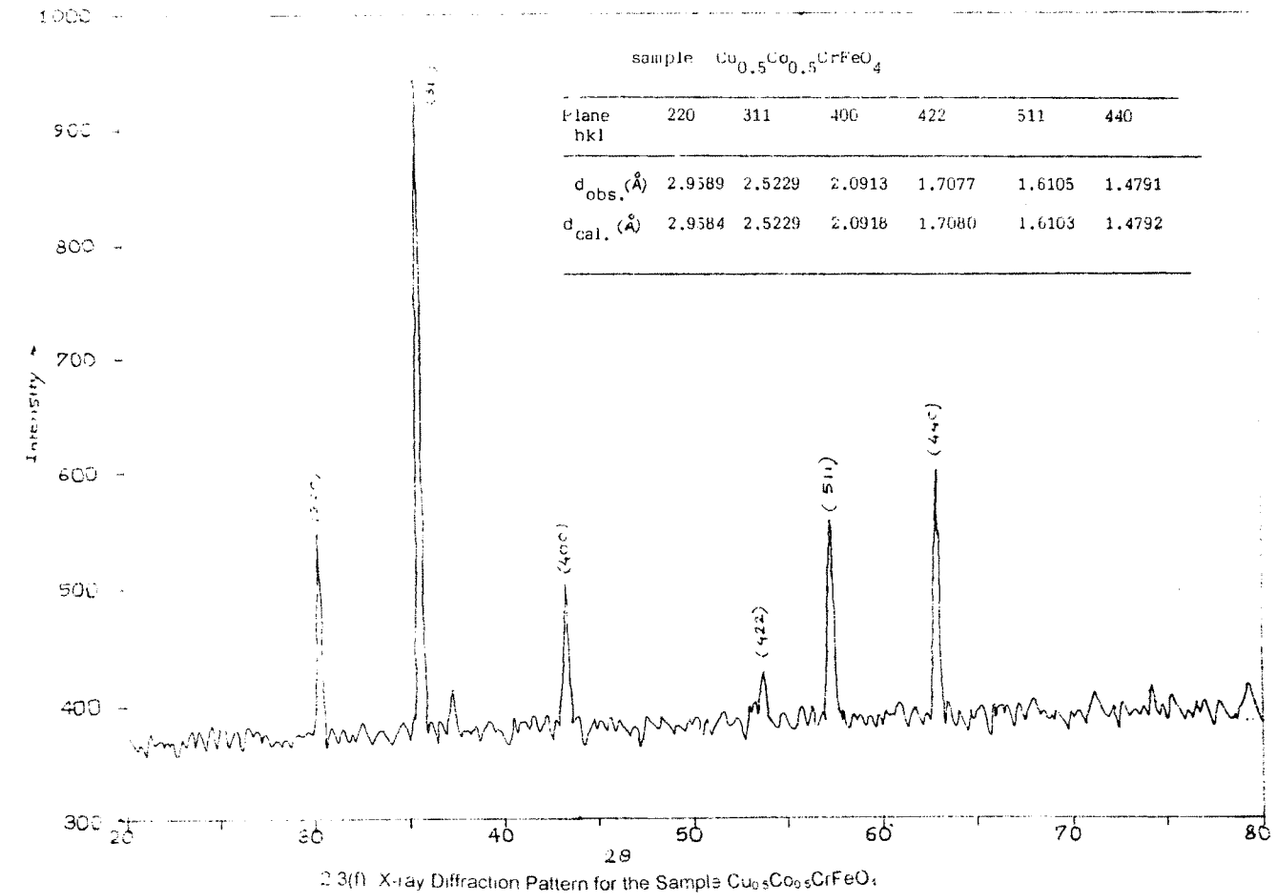

2.3(f) X-ray Diffraction Pattern for the Sample $Cu_{0.5}Co_{0.5}CrFeO_4$

Table 2.1 : Compositional Variation of molecular weight, packing density X-ray density and porosity of $Cu_{0.5}Co_{0.5}Cr_xFe_{2-x}O_4$ Systtem

Composition	Molecular weight	Packing density D_s gm/cm^3	X-ray density D_x gm/cm^3	Porosity $P_o = \frac{D_x - D_s}{D_x} \times 100$ %
$Cu_{0.5}Co_{0.5}Fe_2O_4$	236.9312	4.1405	5.3385	22.44
$Cu_{0.5}Co_{0.5}Cr_{0.2}Fe_{1.8}O_4$	236.161	4.1437	5.3752	22.91
$Cu_{0.5}Co_{0.5}Cr_{0.4}Fe_{1.6}O_4$	235.3908	4.1336	5.3351	22.52
$Cu_{0.5}Co_{0.5}Cr_{0.6}Fe_{1.4}O_4$	234.6206	4.2266	5.3434	20.90
$Cu_{0.5}Co_{0.5}Cr_{0.8}Fe_{1.2}O_4$	233.8504	4.2355	5.3076	20.20
$Cu_{0.5}Co_{0.5}Cr\ FeO_4$	233.0802	4.2403	5.2858	19.78

Table 2.2 : Compositional Variation of Lattice constant and bond lengths of $Cu_{0.5}Co_{0.5}Cr_xFe_{2-x}O_4$ system

X	0.0	0.2	0.4	0.6	0.8	1.0
a_o (A^o)	8.3853 ±0.0029	8.3689 ±0.0023	8.3571 ±0.006	8.3543 ±0.0022	8.3650 ±0.004	8.3672 ±0.0013
RA (A^o)	1.9026	1.8989	1.8962	1.8956	1.8980	1.8985
RB (A^o)	2.0460	2.0420	2.0391	2.0385	2.0411	2.0416

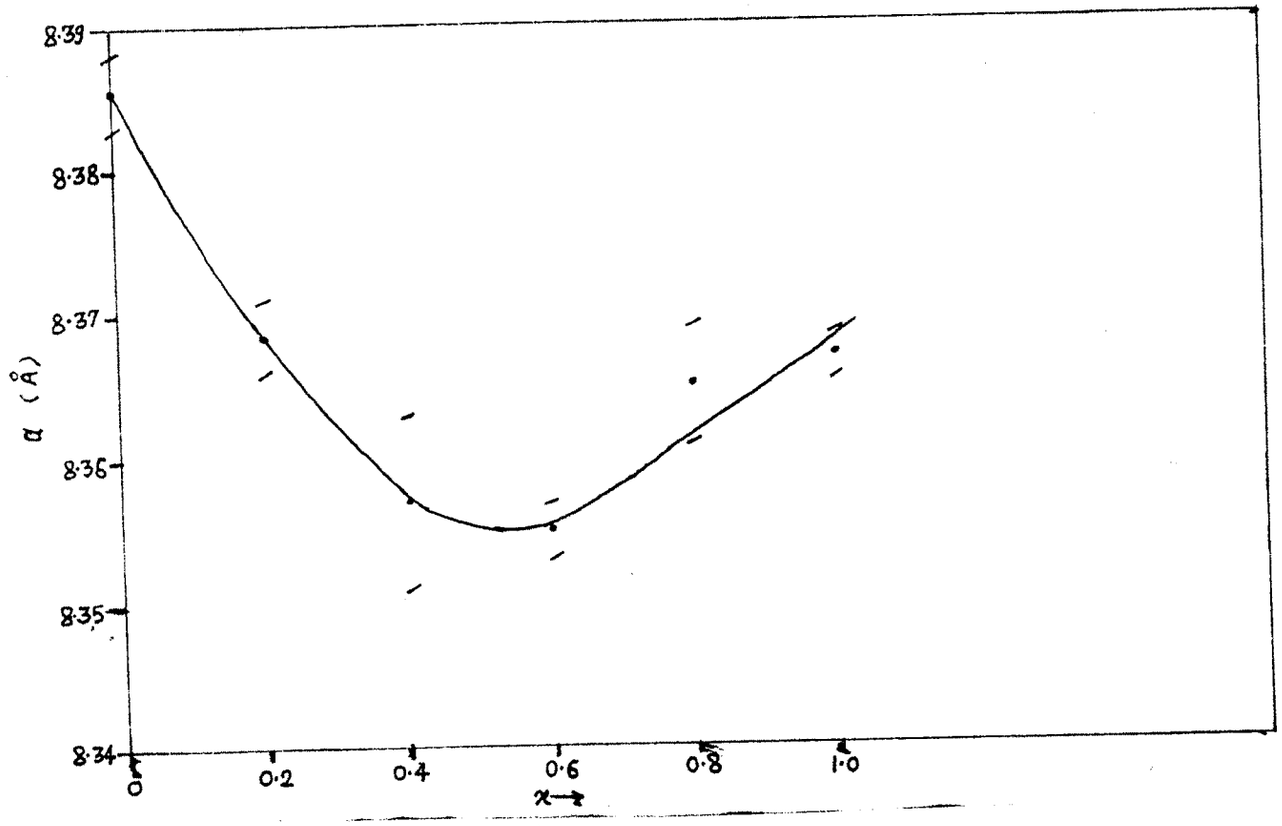

2.4 Compositional Variation of Lattice Constant with x.

The lattice parameter 'a' and bond lengths R_A and R_B determined for different compositions of the system are given in Table (2.2). From the table and also from Fig.(2.4) it is observed that the lattice constant, decreases upto x < 0.6, reaches minimum for x = 0.6 and increases for x > 0.6 Cr. The variation of lattice constant with Cr can be explained on the basis of ionic radii of the substituting elements. The ionic radius of Cr is 0.61 A and that of Fe 0.67 A°. In the present system Fe is replaced by C_r and as can be expected the lattice constant should decrease. The variation of lattice constant follows this trend upto x = 0.6 Cr. However, it is not true for higher contents of Cr. For higher contents of the lattice constant shows an increasing behaviour.

Lattice distortion due to John Tailor ions (Cr, Cu) in spinels has been extensively worked out by Goodenough [14]. Delorme [13] has explained the lattice distortion in $Cu_{1-x}M_xFe_2O_4$, where M = Ni,Mg,Co. According to his study on CuCo ferrites the lattice distortion vanishes at x = 0.4 Co. Otari, et al [15] have carried out the lattice distortion study on the same system and they observed that the lattice distortion vanishes at x = 0.6 Co.

In the present system we have observed the cubic structure for $Cu_{0.5}Co_{0.5}Fe_2O_4$ ferrite. This variation in lattice parameter may be due to slightly different temperature of preparation of ferrites moreover, the temperature and oxidation conditions were different for Co and Cu ferrites.

According to Goodenough the ions such as Cu and Cr occupy at B site and the covalent bond formation (dsp^2) takes place on B site. This bond formation gives rise to lattice distortion. Therefore, in present system the

increase in the lattice constant above x > 0.6 Cr may be due to the distortion caused by Cr and Cu ions at B site.

REFERENCES

1 Patil K.C. and Sunder Manoharan S., Hand book of Ceramics and composits Vol.1 Synthesis and properties Edited by Nicholas P.Chermision of Publ. Marcell Dekker Inc. New York (1990).

2 Standley K.J., Oxide magnetic materials Chap-2 p.9, Cleorendon Press, New York (1972).

3 Economus G.J., Am.Ceram.Soc., 88 (1955) 241.

4 Wolf W.P., Rodrigue G.P.,Appli. Phys. 29 105 (1958)

5 Sato t: IEEE Trans Mag 6 : 708 (1970).

6 Sato T, Kuroda C., Saito M., Ferrites proc. Int.Conf.Kyoto Tokyo press. p.72 (1970).

7 Sunder Manohran S. and Patil K.C., Proceedings of ICF-5 (India) (1989)43

8 Wagner C.Z.,Phys.Chem. B-34(1936) 309-16.

9 Parikov V.V.,Bashikov L.A.,J.Solid State (U.S.A.) Vol.39, No.3 (Oct.1981),398-408.

10 Hendricks S.B., Jafferson M.E.,J.Optical Soc.Am. 23(1933) 299.

11 Bragg W.L. , Nature (London),95 (1915) 561.

12 Cullity B.D., Elements of X-ray diffraction Addison Wesley Publ. Co.England (1959).

13 Debrme C.,Thesis Grenoble (1956).

14 Good Enough J.B.,Loeb A.L., Phys. Rev. 98, 391(1955).

15 Otari S.M. Kadam V.B.,Sawant S.R.Patil S.A., Indian J. of the Pure and Appl.Phys. 28 (1990) 248.